HYDRAULIC STABILITY ANALYSIS OF LEESIDE SLOPES OF OVERTOPPED BREAKWATERS

by

MARUTI D. KUDALE

and

NOBUHISA KOBAYASHI

RESEARCH REPORT NO. CACR-95-10

JULY, 1995

CENTER FOR APPLIED COASTAL RESEARCH
DEPARTMENT OF CIVIL ENGINEERING
UNIVERSITY OF DELAWARE
NEWARK, DELAWARE
19716

ABSTRACT

The hydraulic stability of armor units on the leeside slope of an overtopped breakwater is analyzed using the velocity and depth of overtopping water on the crest computed by an existing numerical model. The structure with its crest at or above the still water level (SWL) under the attack of normally incident wave trains has been considered. The stability analysis is carried out considering the hydrodynamic forces of the overtopping jet impinging on a leeside armor unit. A traditional force balance method is used to predict the stability number N_s for initiation of armor movement. The computed critical stability numbers N_{sc} for stones compare well with the observed stability numbers, provided that the hydrodynamic force coefficients are calibrated once for the stone stability on leeside slopes.

Furthermore, the relative importance of the factors affecting the stability of leeside armor units has been assessed using the calibrated model. Factors considered are 1) crest height above SWL relative to the incident significant wave height 2) seaward and leeside slopes of the breakwater 3) toe depth relative to the incident significant wave height 4) crest width of the breakwater 5) peak period of the incident wave spectrum. The computed stability numbers as a function of the normalized crest height are presented for various combinations of these factors. The minimum stability of leeside armor units occur at the intermediate crest heights. However, as the seaward slope is made flatter, the stability of leeside armors improves. The leeside slope of a breakwater in relatively deeper water is more stable. The leeside stability of a breakwater in shallower water with its crest height near SWL can be improved by steepening the back slope. A wider crest also improves the leeside stability.

Further studies are required to refine the armor stability model. The influence of tailwater in reducing the water velocity of overtopping jet has not been considered in the present analysis.

ACKNOWLEDGEMENT

The study is carried out during the fellowship training of the first author at the University of Delaware. The fellowship was sponsored by the United Nations Development Programme (UNDP) under the Project IND/90/038 at the Central Water and Power Research Station, Pune, India.

Contents

List of Figures

List of Tables

1.0 : INTRODUCTION

Low-crested breakwaters are usually constructed when only partial protection from waves is required landward of breakwaters. Low-crested breakwaters are more economical. Also, a significant amount of wave energy is transmitted due to overtopping, which results in the reduction of wave energy actually dissipated on the seaward slope of the breakwater. The weight of the armor units on the seaward slope can be reduced significantly by allowing overtopping. However the armor units on the crest and leeside slope become vulnerable under overtopping waves. The weight of these armor units may need to be increased to withstand the forces of overtopping water.

The stability of a traditional non-overtopped rubble mound breakwater depends primarily upon the stability of individual armor units on its seaward slope. A major factor in the design of rubble mound breakwaters is hence the minimum weight of the armor units on the seaward slope, required to withstand the design waves. Many studies were carried out on the hydraulic stability of individual armor units on the seaward slope. Several empirical formulae such as Van der Meer formula (1988) are available for the estimation of the minimum weight. The present practices for the design of rubble mounds are based on hydraulic model tests and empirical formulae. A few numerical models have also been developed recently for the design of rubble mound structures. Kobayashi et al. (1989, 1994) developed a numerical model for the design of coastal rubble mound structures, which predicts wave reflection, runup and armor stability on the seaward slope.

For low-crested overtopped rubble mound breakwaters, the stability of leeside armor units also becomes an important design aspect. A few studies have been reported on this design aspect. Lording et al. (1971) suggested that proper considerations should be given to the leeside slope while designing overtopped breakwaters. Walker et al. (1975) indicated that the leeside slope was subjected to more damage than the seaward slope. Wave rundown on the seaward slope is reduced due to overtopping and the weight of the armor units may be significantly reduced as suggested empirically by Van der Meer (1988). However, armor units on the crest and leeside slope are more exposed to the wave forces and their weight may need to be increased. Ahrens et al. (1990) suggested that the increased stability of the seaward slope and the decreased stability of the crest and leeside slope could lead to

stability minimum of the entire structure at an intermediate crest elevation. Van der Meer et al. (1992) proposed simple empirical formulae for different damage levels for the design of leeside armor of berm breakwaters. Anderson et al. (1992) carried out a hydraulic stability analysis of leeside armor for berm breakwaters and suggested a semi-empirical formula for the size of leeside stone. In their analysis, the velocity of overtopping water on the crest was estimated using an empirical formula for wave runup and only the stability of armor units slightly above SWL was analyzed. Losada et al. (1992) used the velocity obtained from the numerical model of Kobayashi et al. (1987, 1989) and showed that the minimum armor stability on the crest occurred when the crest level of a submerged breakwater was at the mean water level. Vidal et al. (1992) carried out random wave tests in a three dimensional wave basin and presented the stability curves for different portions of a low-crested breakwater. The stability number plotted as a function of the normalized crest height showed that the minimum armor stability against the initiation of damage on the leeside slope occurred at an intermediate crest height.

In the present study, the stability of the leeside armor units is analyzed considering the drag, inertia and lift forces caused by the overtopping jet of water impinging on the leeside slope above or below the still water level. The numerical model RBREAK2 by Kobayashi et al. (1994) is used to compute the temporal variations of the horizontal velocity and thickness of the overtopping jet on the crest. The jet of water issuing from the crest is treated as a free jet in a quasi-steady manner. The stability of leeside armor units is expressed in terms of the stability number, N_s as a function of the impinging jet velocity and direction as well as the leeside slope. The computed stability number is shown to be in good agreement with the measured stability number for the initiation of damage presented by Vidal et al. (1992). The stability model is then used to perform sensitivity analyses to gain insight into the mechanisms of the leeside armor stability.

2.0 : ARMOR STABILITY MODEL

2.1 Overtopping Flow on Crest

Kobayashi et al. (1986, 1987) developed a numerical flow model to predict the flow characteristics on rough slopes for specified normally incident wave trains. The wave motion on the slope of a structure is described by the one-dimensional finite-amplitude, shallow water equations including the effect of bottom friction. An explicit dissipative Lax-Wendroff finite difference method is used to solve these equations. This numerical flow model was extended to predict the temporal variations of the velocity and depth of the overtopping flow on the crest of the structure by Kobayashi et al. (1989). The velocity and depth of the overtopping jet at the landward edge of the crest are the input to the stability analysis of leeside armor units presented in this report. The numerical model called RBREAK2 (Kobayashi et al. 1994) for random waves is used for the computations made herein.

2.2 Free Jet Impinging on Leeside Slope

Walker et al. (1975) depicted three possible causes of the failure of the leeside of a low-crested breakwater. 1) pore pressure induced by waves striking the seaward slope 2) overtopping jet of water impinging on the slope and 3) toe scouring of the leeside slope by the impinging jet. Out of these causes the impinging jet on the leeside slope appears to be the most common. The wave-induced pore pressure would be significant only for a porous breakwater with a small width and porous material near the still water level. The toe scouring of the leeside slope may be important in very shallow water but is beyond the scope of this study. The breakwater is assumed to be essentially impermeable and only the stability of leeside armor units under the impinging jet is considered in the following.

The jet of overtopping water issuing from the landward edge of the crest impinges on the leeside slope. The jet may directly hit the leeside slope above SWL as shown in Figure 1 or it plunges into the tailwater and then attacks the leeside slope as shown in Figure 2. The properties of jet striking the leeside slope are analyzed using the following symbols shown in Figures 1 and 2:

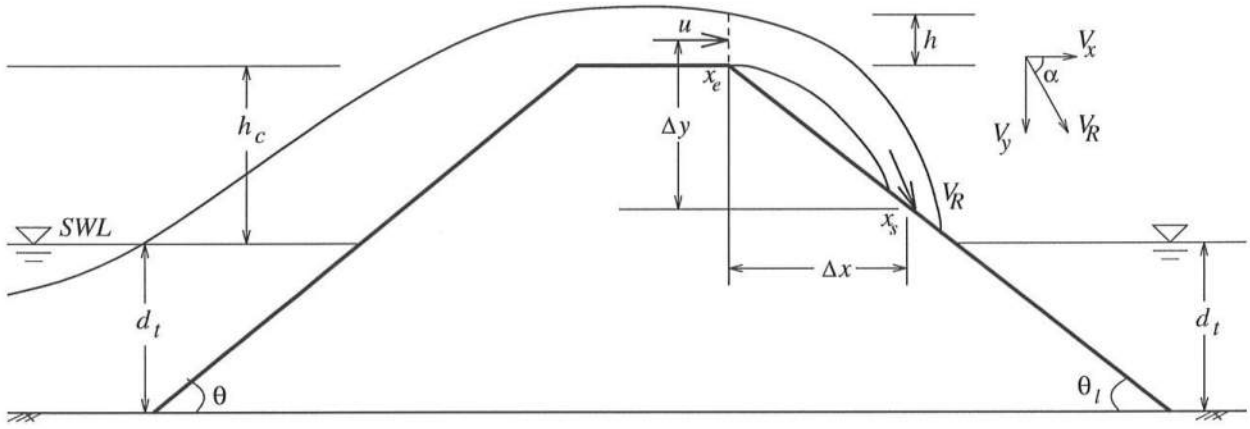

Figure 1: **Jet of Water Impinging on Leeside Slope Above Tailwater Surface**

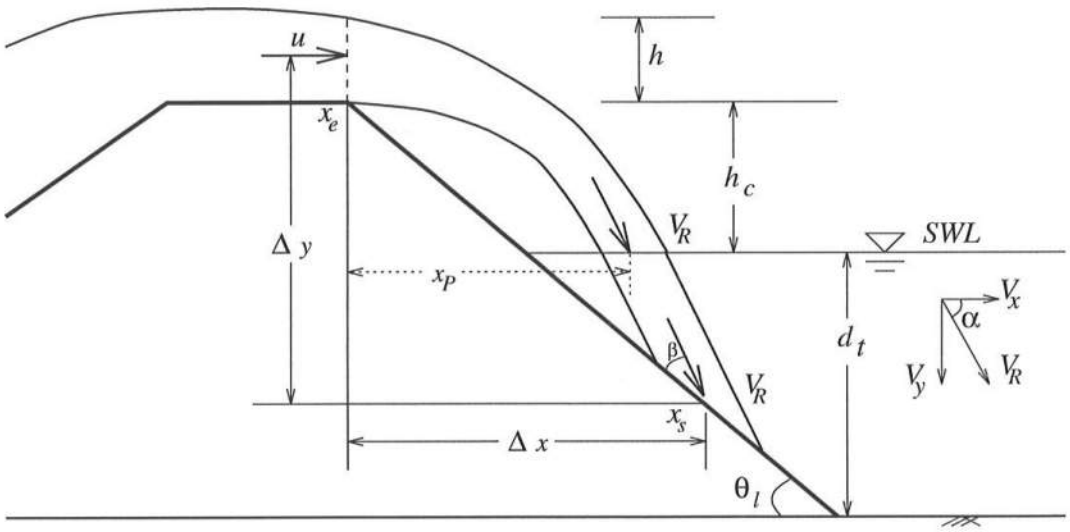

Figure 2: **Jet of Water Impinging on Leeside Slope Below Tailwater Surface**

x_e = landward edge of the breakwater crest

x = horizontal coordinate taken to be positive landward with $x = 0$ at x_e

y = vertical coordinate taken to be positive downward
with $y = 0$ at the center of the overtopping jet at x_e

t = time

d_t = water depth below SWL at the seaward toe of the breakwater
which is assumed to be the same as the tailwater depth

θ = seaward slope angle of the breakwater

θ_l = leeside slope angle of the breakwater

u = depth-averaged horizontal velocity of the overtopping water
at x_e computed by RBREAK2

h = thickness of the overtopping jet at x_e computed by RBREAK2

h_c = crest height of the breakwater above SWL

x_s = impinging point of the jet on the leeside slope

Δx = horizontal distance between the crest edge and the point x_s

Δy = vertical distance between the center of the jet at x_e and the point x_s

V_x = horizontal water velocity of the jet at x_s

V_y = vertical water velocity of the jet at x_s

V_R = resultant velocity of the jet striking the slope at x_s

α = angle of V_R with the horizontal at x_s

β = angle of V_R relative to the leeside slope given by $\beta = \alpha - \theta_l$

The jet of thickness h issuing from the crest with the computed horizontal velocity of u is assumed to fall freely due to gravity. The initial vertical velocity is zero. The horizontal velocity of the freely falling jet remains to be the initial value u if air friction is neglected. However, the vertical velocity accelerates under the influence of gravity and the vertical acceleration is assumed to be the same as the gravitational acceleration g until the jet impinges on the leeside slope above SWL or the tailwater surface. In the following the unknown values of V_R, α, Δx and Δy are expressed in terms of the known values of u, h, θ_l and h_c.

For the case of the jet impinging on the leeside slope above SWL, a simple analysis of the quasi-steady jet falling freely due to the gravitational acceleration g yields the following expressions:

$$V_x = u \tag{1}$$

$$\Delta x = g^{-1}\left[u^2 \tan\theta_l + \left(u^4 \tan^2\theta_l + ghu^2\right)^{1/2}\right] \tag{2}$$

$$\Delta y = \Delta x \tan\theta_l + \frac{h}{2} \tag{3}$$

$$V_y = \frac{g\Delta x}{u} \tag{4}$$

$$V_R = \left(V_x^2 + V_y^2\right)^{1/2} \tag{5}$$

$$\alpha = \tan^{-1}\left(\frac{V_y}{V_x}\right) \tag{6}$$

where the impinging point x_s in Figure 1 can be found from the calculated values of Δx and Δy.

If the point x_s is located below SWL, the jet plunges into the tailwater first and then strikes the leeside slope below SWL. For this case, the jet follows the path of a projectile up to the water surface only. After entering the tailwater, the jet is not falling freely due to gravity. It may be assumed as a first approximation that the jet penetrates straight with the same velocity as the jet velocity at the free surface. Blaisdell and Anderson (1988) made a similar assumption for their analysis of scour at cantilevered pipe outlets. The horizontal distance Δx from the crest edge to the impingment point on the leeside slope is the sum of the free-fall distance x_p to the entry point at the water surface and the horizontal distance of the straight jet penetration below the tailwater surface. The expression for Δx is obtained geometrically using Figure 2.

$$\Delta x = x_p + \frac{(x_p \tan\theta_l - h_c)}{\tan\alpha - \tan\theta_l} \tag{7}$$

where the horizontal distance x_p of the free fall is

$$x_p = u\sqrt{\frac{2(h_c + h/2)}{g}} \tag{8}$$

The vertical velocity V_y at the impinging point x_s in Figure 2 is assumed to be the same as the vertical velocity of the jet at the entry point at the free surface.

$$V_y = \frac{gx_p}{u} \tag{9}$$

The horizontal velocity V_x at the point x_s is assumed to be the same as u and given by (1). The values of Δy ,V_R and α are given by (3), (5) and (6), respectively.

The assumption of the constant jet velocity below the tailwater surface may be reasonable for a short penetration distance and result in the overestimation of the jet velocity at the impinging point x_s for a long penetration distance. It is noted that if the horizontal distance Δx calculated by (7) exceeds the horizontal extent of the leeside slope, the jet will impinge on the seabed but the toe scour landward of the leeside slope is not analyzed herein.

2.3 Hydrodynamic Forces and Armor Stability

The hydrodynamic forces acting on an individual armor unit on the leeside slope are the drag, lift and inertia forces. These forces may be expressed by the following Morison-type equations:

$$Drag\ \ Force; \qquad F_D = \frac{1}{2}\rho C_D C_2 (d)^2 V_R^2 \tag{10}$$

$$Lift\ \ Force; \qquad F_L = \frac{1}{2}\rho C_L C_2 (d)^2 V_R^2 \tag{11}$$

$$Inertia\ \ Force; \qquad F_I = \rho C_M C_3 (d)^3 \left(\frac{dV_R}{dt}\right) \tag{12}$$

where

ρ	= fluid density which is assumed constant
C_D, C_L and C_M	= drag, lift and inertia coefficients
C_2 and C_3	= area and volume coefficients of the armor unit
d	= characteristic length of the armor unit
$\frac{dV_R}{dt}$	= acceleration of the impinging water

The drag force is assumed to act in the direction of the impinging jet as shown in Figure 3. The acceleration of the jet falling freely is vertically downward and its magnitude equals the gravitational acceleration g. The corresponding inertia force acting vertically downward is given by (12) with $dV_R/dt = g$. On the other hand, the inertia force is assumed to be zero where the impinging point x_s is located below SWL. This assumption is consistent with the assumption of the constant jet velocity below the tailwater surface. For simplicity, it may be assumed that the lift force acts upward normal to the slope.

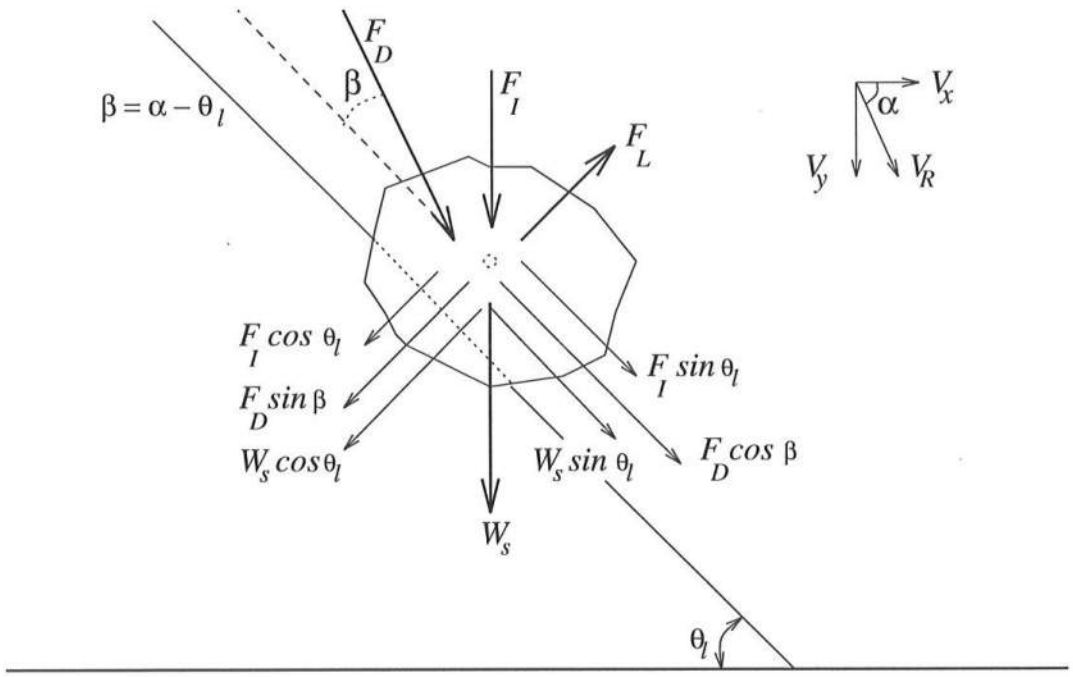

Figure 3: **Forces Acting on Armor Unit**

In addition to these hydrodynamic forces, the submerged weight of the armor unit acts vertically downward.

$$Submerged\ Weight; \qquad W_s = \rho g(s-1)C_3(d)^3 \tag{13}$$

where s = specific density of the armor unit, which is assumed to be fully submerged.

These forces acting on the armor unit may be resolved in the directions parallel and normal to the slope as shown in Figure 3. The static stability condition against sliding or rolling may be given by

$$F_D\cos\beta + F_I\sin\theta_l + W_s\sin\theta_l \;\leq\; (F_D\sin\beta + F_I\cos\theta_l + W_s\cos\theta_l - F_L)\tan\phi \tag{14}$$

in which ϕ = angle of repose of the armor units.

The stability of armor units is traditionally expressed in terms of the stability number, N_s, defined as

$$N_s = \frac{H_s}{(s-1)D_{n50}} \qquad ; \qquad D_{n50} = C_3^{1/3}d \tag{15}$$

where D_{n50} is the nominal diameter defined as $D_{n50} = (M_{50}/\rho s)^{1/3}$ with M_{50} being the median (50% exceedance) mass of the stones. Accordingly, the characteristic armor length d is taken as the length corresponding to $M_{50} = C_3\rho s d^3$. The wave height in (15) is generally taken as the significant wave height H_s.

Substitution of (10), (11), (12) and (15) with $dV_R/dt = g$ or 0 into (14) yields

$$N_s \;\leq\; N_R = \frac{E_3 - E_1}{1+E_2} \tag{16}$$

with

$$E_1 = \frac{2C_3^{2/3}\sin\theta_l}{C_2C_D(\cos\beta - \sin\beta\tan\phi)V_*^2}\left[\frac{C_M}{(s-1)}+1\right] \tag{17}$$

$$E_2 = \frac{C_L}{C_D}\frac{\tan\phi}{(\cos\beta - \sin\beta\tan\phi)} \tag{18}$$

$$E_3 = \frac{2C_3^{2/3}\cos\theta_l\tan\phi}{C_2C_D(\cos\beta - \sin\beta\tan\phi)V_*^2}\left[\frac{C_M}{(s-1)}+1\right] \tag{19}$$

$$V_* = \frac{V_R}{\sqrt{gH_s}} \tag{20}$$

where V_* is the impinging jet velocity normalized by the significant wave height. Eqs. (17) and (19) correspond to the case of $dV_R/dt = g$. For the case of $dV_R/dt = 0$ below the tailwater surface, E_1 and E_3 are given by (17) and (19) without the term $C_M/(s-1)$.

The temporal variations of u and h on the crest for the specified incident wave duration are computed using the numerical model RBREAK2 for the specified geometry of the seaward slope and crest as well as the specified incident wave train. For the specified geometry of the leeside slope, (1)-(9) are used to to calculate the location of the jet impinging point x_s and the impinging velocity V_R and its direction α at each instant when the computed u and h are stored. The value of N_R at that instant is computed using (16). The critical stability number, N_{sc} for the initiation of armor movement is defined as the minimum value of N_R during the entire duration of the incident wave action.

To perform sensitivity analyses, substitution of (17)-(19) into (16) yields

$$N_s \leq N_R = \frac{2C_3^{2/3}\sin(\phi-\theta_l)}{C_2 V_*^2\left[C_L\sin\phi + C_D\cos(\phi+\alpha-\theta_l)\right]}\left[\frac{C_M}{(s-1)}+1\right] \tag{21}$$

Assuming that C_2, C_3, ϕ, C_L, C_D, and s are constant and C_M is constant but zero if point x_s is below SWL, (21) clearly shows the increase of N_R and hence N_s with the increase of C_3 and C_M and the decrease of C_2, C_L and C_D. Also the leeside slope angle θ_l can be adjusted to increase N_R and hence N_s.

There are only two hydrodynamic variables in (21) :

1) $V_* = V_R/\sqrt{gH_s}$ with the jet impinging speed V_R at point x_s

2) α = jet angle at point x_s

Eq. (21) clearly indicates the increase of N_R and hence N_s as V_* decreases and α increases. However, if $\alpha \leq \theta_l$, the jet will not strike the leeside slope. For the jet to strike the leeside slope, α should be greater than θ_l as shown in Figures 1 and 2. This implies that the increase of the leeside slope angle θ_l increases α and increase N_s. The increase of θ_l, however, will also decrease $\sin(\phi-\theta_l)$ and increase $cos(\phi+\alpha-\theta_l)$ where $\phi > \theta_l$ for the stone stability. In addition, V_R^2 is proportinal to u^2 and can be reduced by reducing u^2 using a wider crest or a gentler seaward (front) slope.

The sensitivity of the stability criterion (21) to the force coefficients and the leeside slope is evaluated using the following basic values:

$C_2 = 0.9$, $C_3 = 0.66$, $\phi = 50°$, $s = 2.65$
$C_D = 0.1$, $C_L = 0.025$, $C_M = 0.1$ (or zero if x_s is below SWL)
$\cot\theta_l = 1.5$, $V_*^2 = 2.0$, $\alpha = 40°$

Figure 4 shows the variations of the stability function N_R with C_D, C_L and C_M where these coefficients are varied one by one from the above basic values. N_R increases with C_M and decreases with C_D and C_L as can also be seen in (21). C_M has a minor effect on the value of N_s. The value of N_s significantly depends upon C_D and C_L in the range of C_D and C_L less than about 0.1. Figure 5 shows the sensitivity of N_R to the leeside slope $\cot\theta_l$. For this example, N_R increases fairly rapidly as the leeside slope becomes gentler.

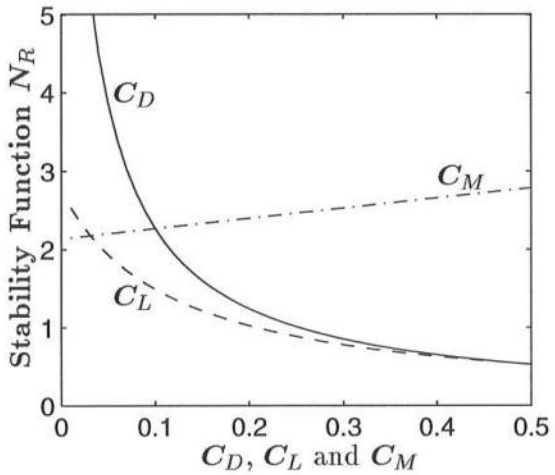

Figure 4: **Sensitivity of Stability Function N_R to Drag, Lift and Inertia Coefficients**

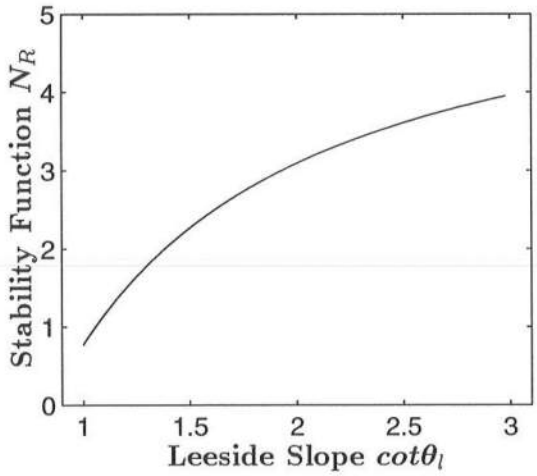

Figure 5: **Sensitivity of Stability Function N_R to Leeside Slope** $\cot\theta_l$

3.0 : COMPARISON WITH AVAILABLE DATA

Vidal et al. (1992) carried out a series of tests in a three-dimensional wave basin for the stability of stones on the seaward slope, crest and leeside slope of a low-crested rubble mound breakwater. The present numerical model is compared with their test data for the initiation of damage on the leeside slope. The characteristics of the tested breakwater were as follows:

seaward slope; $\cot\theta$	= 1.5
leeside slope; $\cot\theta_l$	= 1.5
crest width	= 15 cm
water depth at toe; d_t	= 38 - 60 cm
nominal stones diameter; D_{n50}	= 2.49 cm
specific density of the stone; s	= 2.65

Some of the input parameters for the numerical model are based on those used for the armor stability on the seaward slope computed by Kobayashi and Otta (1987). The friction factor, f', used in RBREAK2 is taken as 0.3 for the seaward slope and crest. The effect of permeability is neglected. The area coefficient, C_2, and the volume coefficient, C_3, of the stone are assumed as 0.9 and 0.66, respectively, and the angle of repose, ϕ, for the stone is assumed to be equal to 50°.

In the numerical model RBREAK2 the input time series of the incident wave train needs to specified at the seaward toe of the structure. The one hour time series based on JONSWAP spectra with its peak period, T_p = 1.4 or 1.8 sec, and its peak enhancement factor, γ =3.3, are used as the input to comply with the wave conditions used in their experiment. The zero moment wave height H_{mo} was varied in their experiment to produce the different damage levels. Four tests in their experiment corresponded to the initiation of damage (ID) on the leeside slope of the low-crested breakwater. The corresponding significant wave height H_s for these four tests is calculated from the observed N_s using (15). Based on these values of H_s the time series of incident wave trains are then simulated numerically using the random phase method for the input to RBREAK2. The conditions of the four ID tests are listed in the rows of test 1-4 in Table 1.

Table 1: **Test Conditions and Stability Numbers**

$Test$ No.	h_c (cm)	d_t (cm)	T_p (sec)	H_{mo} (cm)	H_s (cm)	h_c/H_s	N_s (data)	N_{sc} (computed)
1	0	40	1.4	11.5	11.1	0.00	2.70	2.56
		60	1.4	11.5	11.1	0.00		2.46
2	2	58	1.8	9.1	8.8	0.23	2.15	1.97
		58	1.4	9.1	8.8	0.23		2.20
		38	1.4	9.1	8.8	0.23		1.98
3	4	56	1.4	8.3	8.0	0.50	1.95	2.11
4	6	54	1.4	8.5	8.2	0.73	2.00	2.02
		54	1.8	8.5	8.2	0.73		1.91
5	8	54	1.4	8.5	8.2	0.98	-	2.00
6	10	54	1.4	8.5	8.2	1.22	-	2.02
7	12	54	1.4	8.5	8.2	1.46	-	2.25
8	14	54	1.4	8.5	8.2	1.71	-	2.53
9	16	54	1.4	8.5	8.2	1.95	-	2.80
10	18	54	1.4	8.5	8.2	2.20	-	3.47

Vidal et al. (1992) did not indicate the specific values of d_t and T_p for these four tests. As a result, all the values of d_t and T_p listed in their Table 2 are considered as indicated in the rows of test 1-4 where the first line in each row gives the most likely values of d_t and T_p on the basis of the values of H_{mo} listed in their Table 2. It is noted that test 5-10 listed in Table 1 is hypothetical and used to examine the effect of the crest height h_c greater than the upper limit of $h_c = 6$ cm tested by Vidal et al. (1992). The computed values of N_{sc} are not very sensitive to the differernt values of d_t and T_p used in each test.

The computed time series of u and h at the landward edge of the crest are stored at the rate of 40 points for each spectral period T_p.

The stability model was then calibrated to fit the computed values of N_{sc} with the observed values of N_s for initiation of damage for the leeside slope stones. A good agreement (Figure 6) was obtained with the following values of the force coefficients :

$$C_D = 0.1\ , \quad C_L = 0.025\ , \quad and \quad C_M = 0.1$$

Figure 4 based on (21) suggests that a similar agreement might be obtained using different values of these coefficients. These values of the force coefficients appear to be small as compared to the force coefficients for the stones on the seaward slope of the breakwater calibrated by Kobayashi and Otta (1987). Data on the values of C_D, C_L and C_M for the leeside slope stones will be required to resolve the different values of these coefficients for the seaward and leeside slope stones.

Figure 6 shows the comparison of the computed and observed stability numbers plotted against the normalized crest height, h_c/H_s for test 1-4 listed in Table 1. It can be seen that by adopting the values of the force coefficients as mentioned above, the computed values of N_{sc} for all the four tests are in good agreement with the observed values of N_s.

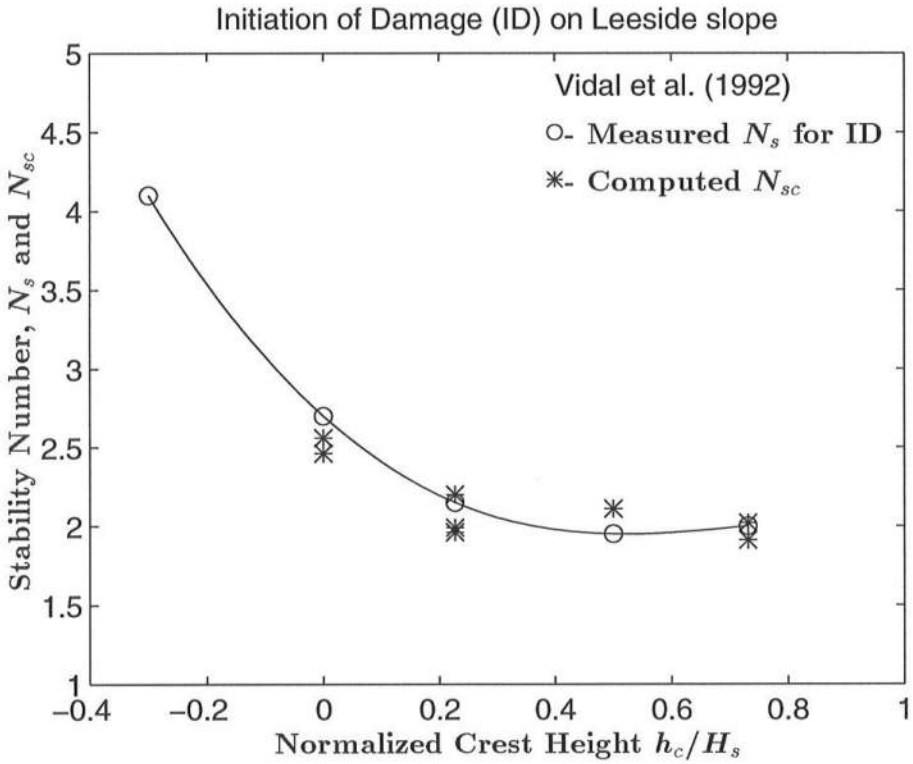

Figure 6: **Comparison of Computed Critical Stability Number N_{sc} with Measured Stability Number N_s for Initiation of Damage (ID) on Leeside Slope as a Function of Normalized Crest Height h_c/H_s**

4.0 : INFLUENCE OF VARIOUS PARAMETERS

In order to study the effect of the increased crest height on the leeside stability above the range tested by Vidal et al. (1992), computations are carried out using the test conditions for test 4 with the crest height being increasesd in an increament of 2 cm as listed as test 5-10 in Table 1. The critical stability numbers for the leeside slopes $\cot\theta_l = 1.25$ and 2 are also calculated for all the tests listed in Table 1 where $\cot\theta_l$ =1.5 in Table 1. Figure 7 shows the variation of N_{sc} with the crest height normalized by H_s for $\cot\theta_l = 1.25$, 1.5 and 2 where the fitted curved line for each slope is added for clarity. For the leeside slope of 1:1.5 the minimum stability occurs at intermediate crest heights. For the leeside slope of 1:1.25, the range of h_c/H_s for the minimum stability is wider. However, for the leeside slope of 1:2, the stability minimum moves towards zero crest height and N_{sc} increases monotonically with the increase of h_c/H_s. Figure 7 also shows that the stability increases rapidly as the crest height is increased beyond the minimum stability range. The stability at zero crest height shows the trend of incresing stability for the negative crest heights, consistent with the computed results by Losada et al. (1992). For this particular case with the normalized depth $d_t/H_s = 6.6$, the armor stability improves significantly as the leeside slope is made flatter.

Computations are also carried out to study the influence of the seaward slope, water depth, crest width and spectral peak period on the leeside armor stability. The basic characteristics of the breakwater and wave conditions chosen for the computations are as follows:

seaward slope; $\cot\theta$	= 2.0
leeside slope; $\cot\theta_l$	= 1.5
crest width	= 15 cm
crest height; h_c	= 0 - 20 cm above SWL
water depth at toe; d_t	= 60 cm
significant wave height; H_s	= 10.0 cm
zero-moment wave height, H_{mo}	= 10.1 cm
peak period T_p of JONSWAP spectrum	= 1.4 sec

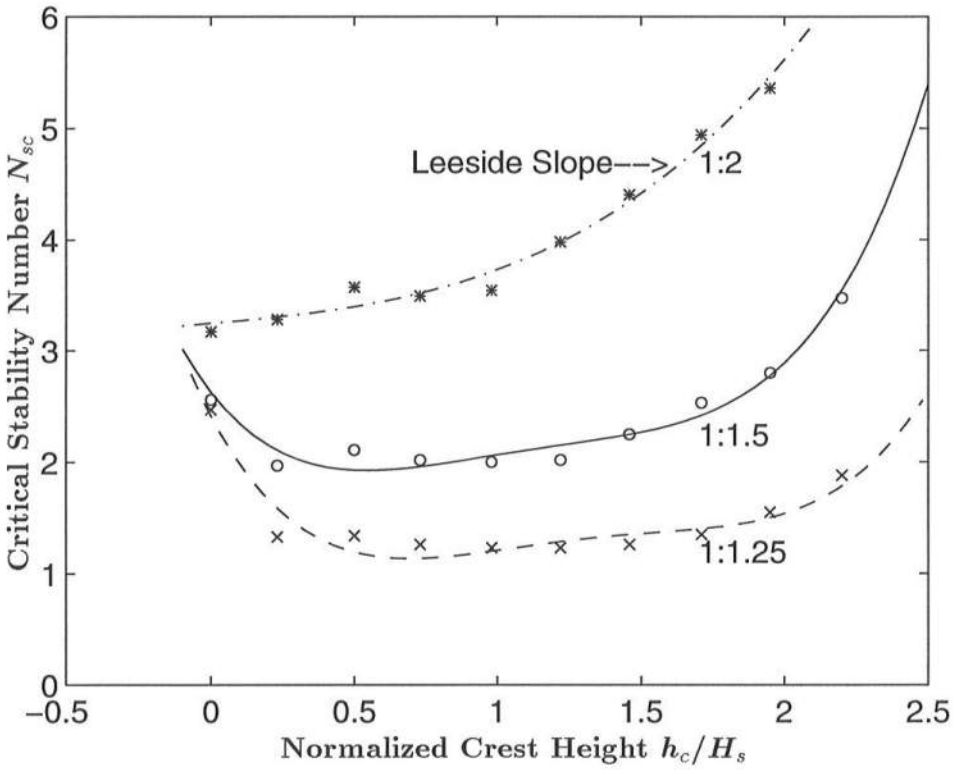

Figure 7: **Computed Variation of N_{sc} with Normalized Crest Height h_c/H_s for Leeside Slopes of 1:1.25, 1:1.5 and 1:2**

The seaward slope $\cot\theta$, the water depth d_t, the crest width and the peak period T_p are varied one by one from these basic values in the following sensitivity anlyses. The values of the critical stability number are computed for different crest heights. However, the computations for the influence of the crest width and peak period are made only for the single crest height of 4 cm above SWL, that is, $h_c/H_s = 0.4$.

Figure 8 shows the influence of the seaward slope on the leeside armor stability where the seaward slope affects the depth-averaged velocity u and the water depth h at the landward edge of the crest computed by RBREAK2. The leeside stability improves as the seaward slope is made flatter. The range of h_c/H_s for the minimum stability becomes smaller and tends to move towards zero crest height for the flatter seaward slope. As the seaward slope becomes flatter, the velocity u of overtopping water is reduced and the stability of leeside armor is increased.

Figure 9 shows the variation of the computed stability number N_{sc} with the water depth at the toe, d_t, normalized by H_s. The stability of the leeside slope is generally larger for the deeper water. However, for the small crest heights at about zero, the leeside armor stability is greater for the shallower water. This is because the overtopping water with the higher velocity for the shallower water impinges beyond the toe of the leeside slope. The intense jet strikes the seabed instead of the leeside armor slope. For the shallower depth the leeside slope stability of a breakwater with a crest near SWL could be increased by increasing the leeside slope angle. However, scour of the seabed landward of the lesside slope may become serious.

Figure 10 shows the variation of the computed stability number N_{sc} with the crest width normalized by H_s. The increase of the crest width of the breakwater improves the stability of the leeside. This is obvious because the increased crest width provides additional friction to the overtopping water on the crest and reduces the velocity u at its landward edge. However, the stability number increases only slowly with the crest width increase and this option may not be very economical.

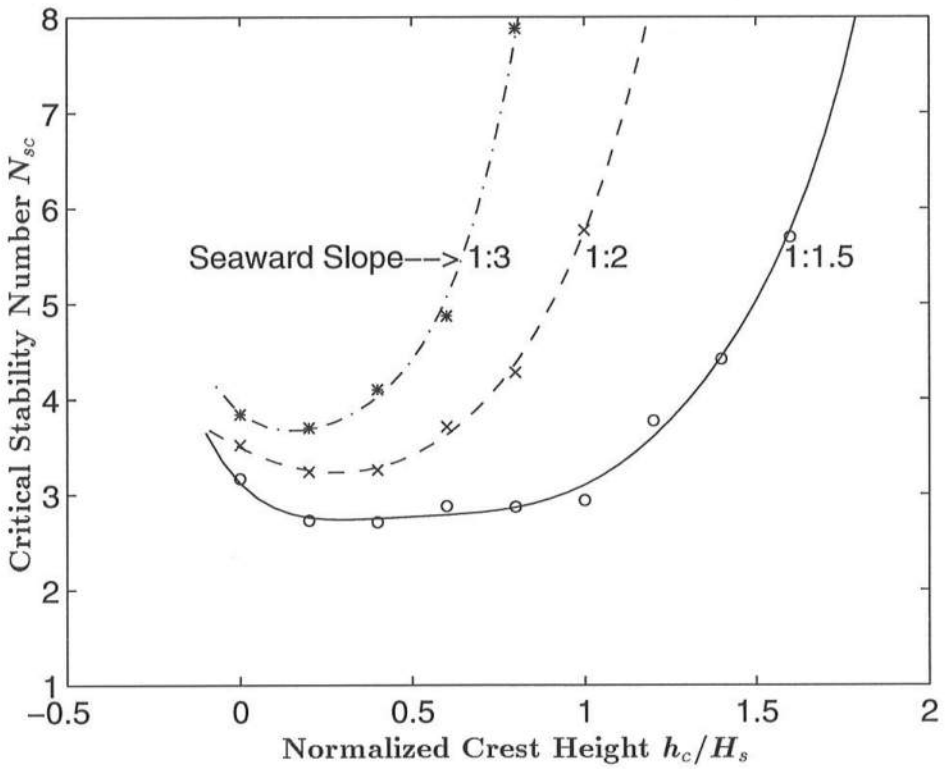

Figure 8: **Computed Variation of N_{sc} with h_c/H_s for Seaward (Front) Slopes of 1:1.5, 1:2 and 1:3**

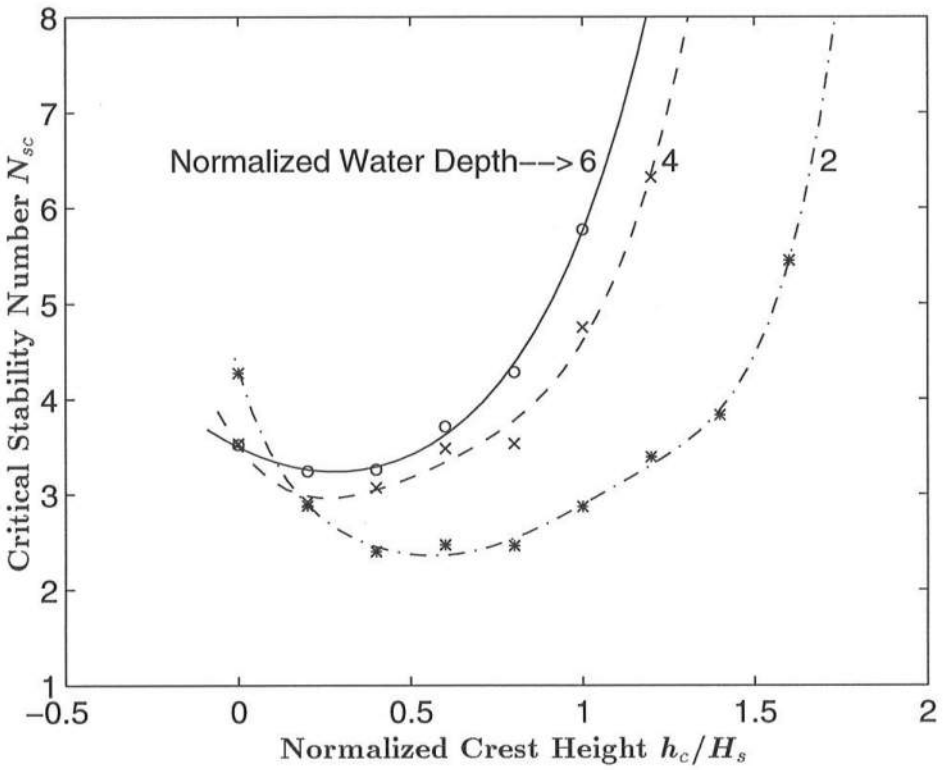

Figure 9: **Computed Variation of N_{sc} with h_c/H_s for Normalized Water Depth d_t/H_s = 2, 4 and 6**

The peak period T_p of the incident wave spectrum has also a noticeable effect on the leeside armor stability. Figure 11 shows the variation of the computed stability number N_{sc} with the Iribarren number ξ defined using the seaward slope $\tan\theta$.

$$\xi = \frac{\tan\theta}{\sqrt{(2\pi H_s) \,/\, (gT_p^2)}} \tag{22}$$

Figure 11 indicates that the stability of the leeside slope decreases with the increasing wave period for this case. The longer period waves increase the overtopping water velocity u for this geometry of the breakwater. A similar result was also observed experimentally by Van der Meer et al. (1992).

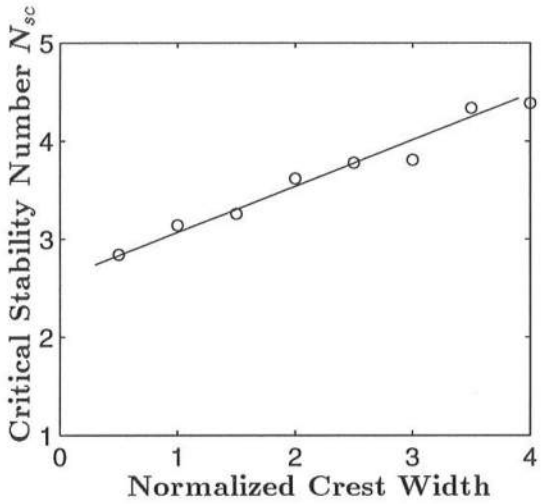

Figure 10: **Computed Variation of N_{sc} with Crest Width Normalized by H_s for $h_c/H_s = 0.4$**

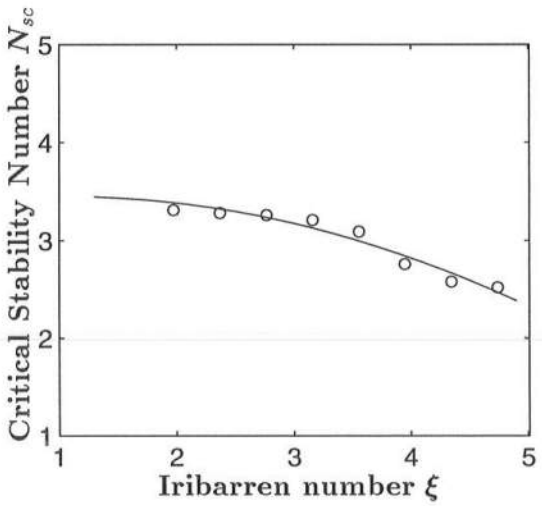

Figure 11: **Computed Variation of N_{sc} with Iribarren Number by Varying Spectral Peak Period T_p for $h_c/H_s = 0.4$**

5.0 : CONCLUSIONS AND RECOMMENDATIONS

A hydraulic stability model for armor units on the leeside slopes of overtopped rubble mound breakwaters has been developed using the water velocity and depth of the overtopping flow computed by the existing time dependent numerical model RBREAK2. A good agreement has been obtained with available limited data. Some of the empirical coefficients used in the model have been calibrated using the same data. Consequently, more extensive data will be required to verify the developed model in a more rigorous manner. The limited computed results presented herein indicate the following qualitative conclusions:

- The flatter leeside slope increases the armor stability.
- The flatter seaward slope of a breakwater improves the leeside armor stability and the crest height for the minimum stability tends to approach zero at SWL for the flatter seaward slopes.
- The leeside slope of a breakwater is more stable in deeper water. Also, the crest height for the minimum stability approaches zero at SWL.
- For relatively shallow water depths the minimum armor stability on the leeside slope occurs for wide intermediate crest heights.
- For the shallower water depths the leeside slope stability of a breakwater with a crest near SWL could be increased by increasing the leeside slope angle.
- The stability of the leeside slope can be improved somewhat by increasing the crest width of a breakwater.

These conclusions are based on the specific computations made in this report. It is difficult to obtain simple general conclusions because the number of parameters involved in this problem is large. The developed hydraulic model will allow one to examine the hydraulic stability of leeside armor units under various wave conditions and breakwater configurations. Consequently, the developed model is very useful in designing the geometry of an overtopped breakwater and the size of leeside armor units.

REFERENCES

Ahrens, J. P. and Cox., J., 1990, 'Design and Performance of Reef Breakwaters', *Journal of Coastal Research*, SI(7), 61-75.

Blaisdell, F. W. and Anderson, C. L., 1988, 'A Comprehensive Generalized Study of Scour at Cantilevered Pipe Outlets', *Journal of Hydraulic Research*, 26(4), 357-376.

Anderson, O. H., Juhl, J. and Sloth, P., 1992, 'Rear Side Stability of Berm Breakwaters', *Proc. 23rd Coastal Engineering Conference*, ASCE, 1020-1029.

Kobayashi, N., Roy, I. and Otta, A. K., 1986, 'Numerical Simulation of Wave Runup and Armor stability', Paper 5088, *18th Offshore Technology Conference*, 1, 51-56.

Kobayashi, N., and Otta, A. K., 1987, 'Hydraulic Stability Analysis of Armor Units', *Journal of Waterway, Port, Coastal and Ocean Engineering*, ASCE, 113(2), 282–298.

Kobayashi, N., and Wurjanto, A., 1989, 'Numerical Model for Design of Impermeable Coastal Structures', *Research Report No. CE-89-75*, Center for Applied Coastal Research, Univ. of Delaware, Newark, Delaware, USA.

Kobayashi, N., and Poff, M. T., 1994, 'Numerical Model RBREAK2 for Random Waves on Impermeable Coastal Structures and Beaches', *Research Report No. CACR-94-12*, Center for Applied Coastal Research, Univ. of Delaware, Newark, Delaware, USA.

Lording, P. T., and Scott, J. R., 1971, 'Armor Stability of Overtopped Breakwaters', *Journal of Waterways, Harbors and Coastal Engineering Division*, ASCE, 97(2), 341-354.

Losada, M. A., Kobayashi, N. and Martin, F. L., 1992, 'Armor Stability on Submerged Breakwaters', *Journal of Waterway, Port, Coastal and Ocean Engineering*, ASCE, 118(2), 207-212.

Van der Meer, J. W., 1988, 'Rock Slopes and Gravel Beaches Under Wave Attack', *Delft Hydraulics Communication No. 396*, Delft, The Netherlands.

Van der Meer, J. W., and Veldman, J. J., 1992, 'Singular Points at Berm Breakwaters: Scale Effects, Rear, Roundhead, and Longshore Transport', *Coastal Engineering*, 17, 153-171.

Vidal, C., Losada, M. A., Medina, R., Mansard, E. P. D. and Gomez-Pina, G., 1992, 'A Universal Analysis for the Stability of Both Low-Crested and Submerged Breakwaters', *Proc. 23rd Coastal Enginering Conference*, ASCE, 1679-1692.

Walker, J. R., Palmer, R. Q. and Dunham, J. W., 1975, 'Breakwater Backslope Stability', *Proc. Civil Engineering in the Oceans*, ASCE, 879-898.

APPENDIX A

LISTING OF
COMPUTER PROGRAM LEESTAB

```
C
C     Program "LEESTAB" for the  'Hydraulic Stability Analysis
C     of Leeside Armor  Units'.  Program computes the Critical
C     Stability Number, Nsc for the armor on leeside  slope of
C     the impermeable rubble mound breakwaters.
C
C     The program uses the values of horizontal  velocity and
C     water depth at the landward edge of the crest, computed
C     by a numerical model  RBREAK2.  The otput file OOVER of
C     RBREAK2 contains the values of m=uh and h, where 'u' is
C     normalized  hurizontal water partical velocity and  'h'
C     is the normalized total water depth below instantaneous
C     water surface elevation.
C
C               Written by M. D. Kudale and N. Kobayashi
C                 Center for Applied Coastal Research
C                   Department of Civil Engineering
C             University of Delaware, Newark, Delaware 19716
C                             April  1995
C
      PROGRAM LEESTAB
C
C     N     = data point
C     NEND  = Total number of data points.
C     NRATE = Rate at which the the time series is stored per
C             wave period, in the data file OOVER
C     TIME(N)  = current normalized time = N/NRATE
C     U1(N)    = Dimensionless volume flux, m=uh
C     U2(N)    = Total water Depth, h
C     VX(N)    = Horizontal velocity, u
C
      PARAMETER (N1=12000)
      DIMENSION U1(N1),U2(N1),VX(N1),VY(N1),VR(N1),SNR(N1)
      DIMENSION DELX(N1),TIME(N1),DELY(N1),ALPHA(N1)
C
      CHARACTER*10 OOVER
C
C     Read data related to armor stability.
C     This data is stored in file FINP3
C
      OPEN (UNIT=13,FILE='FINP3',STATUS='OLD'
     &                  ,ACCESS='SEQUENCIAL')
      READ(13,*)
      READ(13,*)
C
C     C2 = area    coefficient of the armor unit
C     C3 = volume  coefficient of the armor unit
C     CD = drag    coefficient
C     CL = lift    coefficient
C     CM = inertia coefficient
C     SG = specific gravity of the armor unit
C     TANPHI = tan(phi), with phi= frictional angle of armour
C     COTHET = cot(thetal), with thetal = leeside slope angle
C     HC = crest height above SWL normalized by wave height
C     DT = water depth at the toe normalized by wave height
```

```
C     T  = reference wave period
C     00VER is the file contianing data of u and h
C     which are normalized by  wave height H
C
      READ(13,1010)C2,C3,SG
      READ(13,1010)CD,CL,CM
      READ(13,1010)TANPHI
      READ(13,1010)COTHET
      READ(13,1010)HC,DT
      READ(13,1010)T
      READ(13,1020)OOVER
 1010 FORMAT(3F13.6)
 1020 FORMAT(A10)
C
C      Read file OOVER
C
      OPEN (UNIT=63,FILE=OOVER,STATUS='OLD'
     &                ,ACCESS='SEQUENCIAL')
      NRATE = 40
      NEND = (160.0/T)*NRATE
      DO 100 N =1,NEND
        READ(63,1000)U1(N),U2(N)
        IF (U2(N).GT.0.0) THEN
          VX(N) = U1(N)/U2(N)
        ELSE
          VX(N) = 0.0
        ENDIF
 100  CONTINUE
 1000 FORMAT(2E15.6)
C
C     XLIM = horizontal distance between landward edge of
C               crest and the leeward SWL normalized by H
C     HLIM = horizontal distance between landward edge of
C               crest and the leeside toe normalized by H
C
      XLIM = (HC)*COTHET
      HLIM = (HC+DT)*COTHET
C
C     Compute angle 'thetal' from its cotangent
C
      TANTHE =1.0/COTHET
      THETAL = ATAN(TANTHE)
C
C    Compute parameters required for Stability Number.
C
      CST1  = 2.0*(C3)**(2.0/3.0)/(C2*CD)
      CST2  = CM/(SG-1.0) + 1.0
      CSTAB = (CST1*CST2)
      CE2   = CL/CD*TANPHI
C
C     Compute the velocity of jet of water impinging the
C     leeside slope and the distance at which it strikes
C     the slope.    Using this velocity compute critical
C     stability number.
C     The computations are made for each data point.
```

```
C     VX(N)    = Horizontal velocity of jet of water.
C     Horizontal accn. is assumed to be zero.  So VX(N) will
C     not change as the projectile of mass of water proceeds.
C     Vertical velocity will change due to the  influence of
C     gravity.
C     VY(N) = Vertical velocity of jet of water.
C     VR(N) = Resultant velocity when jet strikes the slope.
C     DELX(N) = Horizontal distance between landward edge of
C     crest and the point at which the jet strikes the slope.
C     DELY(N) =  Vertical distance  between center of jet at
C     landward edge of the crest  and the point at which the
C     jet strikes the slope
C     YLIM     = Height of centre of jet at crest from SWL
C     ALPHA(N)= Angle of VR(N) with the horizontal
C
      DO 200  N = 1, NEND
        VSTAN    = (VX(N)**2.0)*TANTHE
        DELX(N) = VSTAN + SQRT(VSTAN**2.0 + U2(N)*VX(N)**2.0)
        DELY(N) = DELX(N)*TANTHE + U2(N)/2.0
        YLIM     = HC + U2(N)/2.0
C
C     If DELY(N) < YLIM then jet strikes the slope above SWL.
C     In this case  VR(N) is computed using equations of the
C     projectile.
C
          IF ((DELY(N)).LE.YLIM) THEN
            VY(N)     = DELX(N)/VX(N)
            VR(N)     = SQRT(VX(N)**2.0 + VY(N)**2.0)
            ALPHA(N) = ATAN(VY(N)/VX(N))
            CE1    = CSTAB*SIN(THETAL)
            CE3    = CSTAB*COS(THETAL)*TANPHI
          ELSE
C     If DELY(N)>YLIM then jet strikes the water surface first.
C     The jet follows the path of projectile  untill it strikes
C     water surface. However, after  entering the water surface
C     it travels in   the same dirction and with  same velocity
C     before entering  the water surface.
C     The horizontal and vertical distance of a point where the
C     jet hits the leeside slope are computed using geometry.
C
            XP        = VX(N)*SQRT(2.0*YLIM)
            XD        = XP-XLIM
            VY(N)     = XP/VX(N)
            ALPHA(N) = ATAN(VY(N)/VX(N))
            XL        = XD*TANTHE/(TAN(ALPHA(N))-TANTHE)
            DELX(N)   = XP + XL
            DELY(N)   = DELX(N)*TANTHE  + U2(N)/2.0
            VR(N)     = SQRT(VX(N)**2.0 + VY(N)**2.0)
            CE1       = CST1*SIN(THETAL)
            CE3       = CST1*COS(THETAL)*TANPHI
          ENDIF
C
C       compute the normalized time
        TIME(N) = FLOAT(N)/FLOAT(NRATE)
C       ANGD = angle at which the jet hits the slope
```

```
          ANGD = ALPHA(N)-THETAL
C
C         Now compute the Stability Number, SNR(N)
C
C         CE =parameter required in stability number computation.
C         Set CE equal to zero if ANGD =< zero,  because in this
C         case the jet will not meet the slope.
C
            IF (ANGD.LE.0.0) THEN
              CE = 0.0
            ELSE
              CE = COS(ANGD) - SIN(ANGD)*TANPHI
            ENDIF
C
C         Set stability number = 100,   if  i) CE = 0.0  or
C         ii) VX(N) = 0.0  or  iii) the jet hits the seabed
C         beyond the landward toe of the breakwater.
C
            IF (CE.LE.0.0.OR.VX(N).EQ.0.0.OR.DELX(N).GT.HLIM)
     &        THEN
              SNR(N) = 100.0
            ELSE
C
C         E1, E2 and E3 are the parameters in stability number.
C
              E1 = (CE1/CE)/VR(N)**2.0
              E2 = CE2/CE
              E3 = (CE3/CE)/VR(N)**2.0
C
              SNR(N) =(E3-E1)/(1.0+E2)
C
C         Set SNR(N) = 100 if it is greater than 100
                IF(SNR(N).GT.100.0) THEN
                  SNR(N) =100.0
                ELSE
                ENDIF
            ENDIF
C
 200    CONTINUE
C
C        find the minimum value of SNR(N)
C
        SNC = SNR(1)
          DO 300 N = 2, NEND
            IF ( SNR(N).LT.SNC) THEN
              SNC = SNR(N)
            ELSE
            ENDIF
 300      CONTINUE
C
          WRITE(*,*)'Critical Stability Number, Nsc = ',SNC
C
        STOP
        END
```

DATA FILE 'FINP3' FOR PROGRAM LEESTAB

(FOR TEST NO. 5 IN TABLE 1)

```
   DATA FILE FOR leestab
   Armor stability parameters
0.900000     0.660000     2.650000    --> C2,C3,SG
0.100000     0.025000     0.100000    --> CD,CL,CM
1.191753                              --> TANPHI
1.500000                              --> COTHET
0.980000     6.585000                 --> HC, DT
1.400000                              --> T
OOVER                                 --> OOVER
```